Numerical study of light-induced drift of Na in noble gases

J. E. M. Haverkort,* H. G. C. Werij,† and J. P. Woerdman
Department of Molecular Physics, Huygens Laboratory, University of Leiden, P.O. Box 9504, 2300 RA Leiden, The Netherlands
(Received 30 November 1987; revised manuscript received 3 May 1988)

We present a model for light-induced drift (LID) in the Na–noble-gas system which should enable direct comparison with experiment. In contrast to previous theories of LID based on a two-level description of the optical absorbers and on a simplified collision treatment, the present model is based on a realistic description of laser-driven Na atoms immersed in a buffer gas. Starting from the generalized Bloch equations, we introduce a rate-equation model for the velocity distributions in the four important Na levels. The velocity-changing and fine-structure-changing collisions are described using composite Keilson-Storer collision kernels in which all adjustable parameters have been eliminated by using available literature data. We apply the model in numerical calculations of LID as a function of all experimentally accessible parameters. It is found that the ground-state hyperfine splitting can have large effects on LID, whereas the excited-state fine-structure splitting has not. The paper establishes criteria for optimum LID effects; when using a single-frequency laser the maximum attainable drift velocity is predicted to be 13.8 m/s. Using a proper set of boundary conditions, we find a pressure dependence of LID qualitatively different from the predictions based on previous work. Finally, the influence of the collision model is investigated. We find that LID is independent of the shape of the collision kernel, indicating that a strong-collision model is always valid.

I. INTRODUCTION

The phenomenon of light-induced drift (LID) can occur when a component of a binary gas mixture is velocity-selectively excited by a traveling laser beam.[1,2] We will consider Na atoms as the active atoms which are immersed in a buffer gas of noble-gas atoms. Due to the velocity-selective excitation, the Na atoms in the excited-state will obtain a nonzero average velocity along the laser beam; the Na atoms in the ground state will obtain a nonzero average velocity in the opposite direction. In the absence of velocity-changing collisions with a buffer gas, these two fluxes of Na atoms will cancel. However, in the presence of a buffer gas, the two fluxes will not compensate when the rate for velocity-changing collisions is state dependent, which is generally the case for states connected through an electronic transition. The net drift flux which results can most easily be understood by noting the difference in mean-free path between excited-state Na atoms and ground-state Na atoms with opposing velocities.

This phenomenon was predicted by Gel'mukhanov and Shalagin[1,2] in 1979. Theoretically, a large number of mainly Soviet papers has been devoted to LID[3–12] and its generalizations.[13–19] The first experimental observation of LID was reported by Antsygin *et al.*[20] for the case of Na in He and Ne. LID in molecular gases such as CH_3F and NH_3 which can be vibrationally excited by a CO_2 laser, has been reported[21] and molecular isotope separation has been demonstrated.[22] Atomic isotope separation has also been demonstrated for the case of Rb.[23,24] A spectacular manifestation of LID was reported by Werij *et al.*[25] who observed an optical piston sweeping Na with a velocity of 1 mm/s through a capillary filled with a noble gas. Such piston has also been observed for the case of Rb by Hamel *et al.*[26] However, even in these experiments, the potential of the LID phenomenon was still hidden by the alkali-wall interaction which slowed down the piston velocity by two orders of magnitude.

Recently, Atutov *et al.*[27] succeeded in eliminating these surface complications by using a paraffin-coated capillary. In a beautiful experiment they observe clouds of Na moving with a speed of 14 m/s through a capillary containing a noble gas. This experiment was named the optical machine gun due to the high repetition rate that could be established; it finally showed that drift velocities of several meters per second, as theoretically expected, could be directly observed experimentally. As demonstrated by Werij *et al.* this set up allowed, for the first time, quantitative measurements of the drift velocity of Na in a noble gas.[28] Also silane-coated capillaries have been shown to be successful in reducing surface complications.[29]

In view of this recent experimental breakthrough, there is a current need for quantitative theoretical calculations of the light-induced drift velocity of alkali-metal atoms in a noble-gas environment. Until recently all theoretical work on LID was of analytical nature, based on a two-level description of the absorbers and/or on a rather simplified collision model (i.e., either weak or strong collisions). Though yielding essential qualitative understanding of the LID phenomenon, this work failed to give quantitative predictions for LID in alkali-metal–noble-gas mixtures. In this paper we will theoretically study LID of Na atoms in noble gases using a rate-equation model which has been recently used to analyze fine-structure changing and velocity-changing collisions of Na atoms.[30] In our model for LID the multiplet struc-

ture of the energy levels of the Na atom is taken into account and collisions are described by a suitable model kernel allowing for collisional interactions in between weak and strong. This leads to a set of rate equations for the velocity distributions of the four energy levels involved; by using available literature data all adjustable parameters have been eliminated. The price to be paid for introducing these more realistic assumptions as compared to previous theoretical work is that the set of equations can only be solved numerically.

II. RATE EQUATIONS DESCRIBING LID

In our description of LID of Na in noble gases we treat the Na atom as a four-level system, which is shown schematically in Fig. 1. We take into account the hyperfine splitting of the $3s\,^2S_{1/2}$ ground state ($\Delta\nu_{\rm hfs}=1772$ MHz), which is of the order of the Doppler width ($\Delta\nu_D=1.6$ GHz) and the fine-structure splitting of the $3p$ excited state. Levels 1 and 2 represent the ground-state $F=1$ and $F=2$ hyperfine levels, respectively. Level 0 represents the excited state which is directly populated by the pump laser and which can be either the $3p\,^2P_{3/2}$ or the $3p\,^2P_{1/2}$ fine-structure level. Level 3 is the nonresonant fine-structure level of the $3p$ excited state, which is not directly populated by the pump laser since the fine-structure splitting (510 GHz) is much larger than the Doppler width. Levels 0 and 3 are coupled by collisions (fine-structure mixing) whereas levels 1 and 2 are not. The hyperfine structure of the excited state is neglected in our model; this may motivated by the fact that under most experimental LID conditions the power- and collision-broadened homogeneous linewidth is larger than the excited-state hyperfine splittings; also Zeeman structure is neglected since the rate of collisional m_F mixing is larger than that of kinetic collisions.

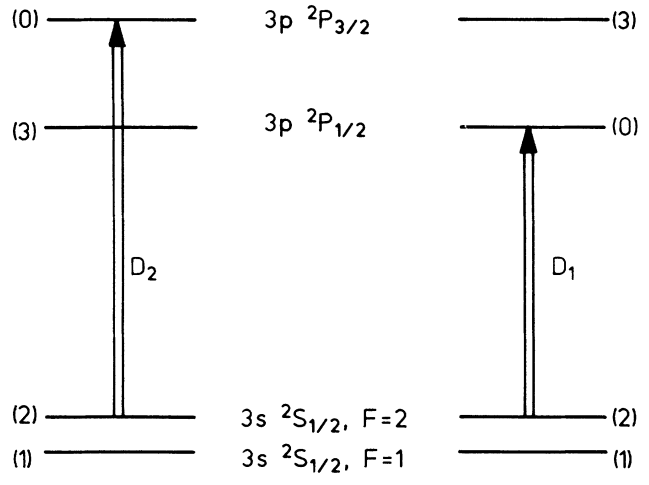

FIG. 1. Simplified energy level diagram of Na. Levels 1 and 2 are the $3s\,^2S_{1/2}$ $F=1$ and $F=2$ ground-state levels, respectively. Levels 0 and 3 are the resonant and nonresonant $3p$ excited-state fine-structure levels, respectively. The $3p$ hyperfine splitting has been neglected. The level numbering is chosen in such a way that level 0 is the $3p\,^2P_{1/2}$ level for D_1 excitation and the $3p\,^2P_{3/2}$ level for D_2 excitation. We have restricted the numerical results shown in Figs. 3–11 to the case of D_2 excitation.

The drift velocity, which is the average velocity of the Na atoms, is given by

$$v_{\rm dr}=\sum_i v_{\rm dr}^{(i)}=\sum_i \int v f_i(v)dv \ , \tag{1}$$

where we sum the first moments of the velocity distributions in the four relevant Na levels. The total velocity distribution defined as $f(v)=\sum_i f_i(v)$ has been normalized to unity, i.e.,

$$\int f(v)dv=1 \ . \tag{2}$$

Starting from the generalized Bloch equation, which describes the evolution of the velocity-dependent density matrix $\rho(\mathbf{v},t)$, we obtain the following set of rate equations for the diagonal elements of the density matrix $[f_i(v)=\rho_{ii}(v)]$:[30]

$$\begin{aligned}
\frac{\partial f_0}{\partial t}=0=&R_{10}\left[f_1-\frac{g_1}{g_0}f_0\right]+R_{20}\left[f_2-\frac{g_2}{g_0}f_0\right]\\
&-Af_0+\mathcal{L}_{00}f_0+\mathcal{L}_{03}^{-}f_0+\mathcal{L}_{30}^{+}f_3\\
&+\Gamma_T[n_0^{(0)}W(v)-f_0] \ ,\\
\frac{\partial f_1}{\partial t}=0=&-R_{10}\left[f_1-\frac{g_1}{g_0}f_0\right]+\alpha_{01}Af_0+\alpha_{31}Af_3\\
&+\mathcal{L}_{11}f_1+\Gamma_T[n_1^{(0)}W(v)-f_1] \ ,\\
\frac{\partial f_2}{\partial t}=0=&-R_{20}\left[f_2-\frac{g_2}{g_0}f_0\right]+\alpha_{02}Af_0+\alpha_{32}Af_3\\
&+\mathcal{L}_{22}f_2+\Gamma_T[n_2^{(0)}W(v)-f_2] \ ,\\
\frac{\partial f_3}{\partial t}=0=&-Af_3+\mathcal{L}_{33}f_3+\mathcal{L}_{30}^{-}f_3+\mathcal{L}_{03}^{+}f_0\\
&+\Gamma_T[n_3^{(0)}W(v)-f_3] \ .
\end{aligned} \tag{3}$$

This set of equations is identical to Eqs. (3.1a)–(3.1d) of Ref. 30. The coherence ρ_{12} is neglected in the present treatment. This is justified when the Rabi frequency Ω is sufficiently small so that the pump laser interacts with two distinct velocity classes in levels 1 and 2 which do not spectrally overlap. It can be shown that this corresponds to the condition $(\frac{1}{2}\Omega^2\ll(\Gamma\Delta\omega_{\rm hfs})$, where $\Gamma=\frac{1}{2}A+\Gamma^{\rm ph}$ is the collision-broadened homogeneous linewidth and $\Gamma^{\rm ph}$ is the rate of phase-perturbing collisions.[31] The finite residence time of the Na atoms inside the laser beam is taken into account by relaxation terms with rates Γ_T which describe the diffusion of Na atoms into and out of the laser beam; the equilibrium atoms outside the laser beam have populations $n_i^{(0)}$ and a Maxwellian velocity distribution $W(v)$ (under experimental conditions thermalization might, for instance, take place at the wall of the vessel). $R_{i0}(v)$ are velocity-selective excitation rates, g_i are degeneracy factors, α_{ij} are branching ratios for spontaneous decay to the ground-state hyperfine levels, and $\mathcal{L}_{ij}$ are operators for velocity-changing and fine-

structure-mixing collisions.

The collision operator $\mathcal{L}$ can be expressed in terms of a collision kernel $K(v \rightarrow v')$, e.g.,

$$\mathcal{L}_{ii} f_i(v) = -f_i(v) \int K(v \rightarrow v') dv' + \int K(v' \rightarrow v) f_i(v') dv' , \quad (4)$$

where the first term on the right-hand side of Eq. (4) is generally written in terms of a rate of velocity-changing collisions, $-\Gamma^{vcc}(v) f_i(v)$. The collision kernels for velocity-changing and fine-structure-mixing collisions in all four levels have been determined through laser-spectroscopic experiments for all Na–noble-gas mixtures.[30] By using a composite kernel made up of Keilson-Storer kernels for large-angle (LA) and small-angle (SA) scattering and by treating fine-structure-mixing collisions in the sudden limit, excellent agreement with measured velocity distributions was obtained. In the one-dimensional case the Keilson-Storer kernel has the form

$$K(v' \rightarrow v) = \Gamma^{KS} \frac{1}{\pi^{1/2} \Delta u} \exp\left[-\left[\frac{v - \alpha^{KS} v'}{\Delta u} \right]^2 \right] , \quad (5a)$$

$$\Delta u = \left[\frac{2 k_B T}{m} [1 - (\alpha^{KS})^2] \right]^{1/2} , \quad (5b)$$

where $0 \leq \alpha^{KS} \leq 1$. We see that the Keilson-Storer kernel has two parameters, a collision rate Γ^{KS} and a strength parameter α^{KS}. After a collision the average velocity is $\alpha^{KS} v'$ and the average velocity spread is Δu. The measured parameters of the Keilson-Storer kernels for LA and SA scattering have been given in Table I of Ref. 30 for all Na–noble-gas pairs. As a result no free parameter is left in the present model for LID in Na–noble-gas mixtures. All radiative and collisional couplings contained in Eqs. (3) are schematically indicated in Fig. 2.

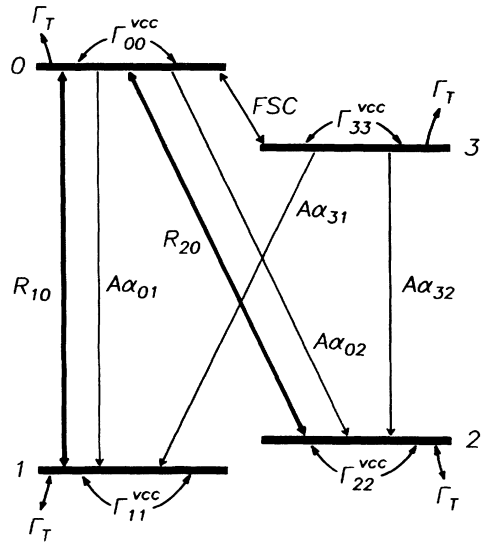

FIG. 2. Radiative and collisional couplings in the simplified four-level scheme of Na. R_{ij} are the rates of velocity-selective excitation, $A\alpha_{ij}$ are the rates of spontaneous decay, Γ_i^{vcc} are the rates of velocity-changing collisions, and Γ_T is the rate of transverse diffusional relaxation. Fine-structure changing collisions are schematically denoted by FSC. Collisional transitions $1 \leftrightarrow 2$ are forbidden.

III. NUMERICAL RESULTS FOR THE DRIFT VELOCITY

In this section we give some representative numerical results for the drift velocity of Na in a noble gas as a function of all experimentally accessible parameters. These results have been obtained by solving numerically the set of rate equations [Eqs. (3)] for the velocity distribution functions in all four relevant levels. The drift velocity has been obtained by calculating the first moment of the total velocity distribution [Eq. (1)]. In the examples we restrict ourselves to the case of excitation on the D_2 transition, i.e., level 0 corresponds to $^2P_{3/2}$ and level 3 to $^2P_{1/2}$.

In the numerical computation we have replaced the continuously variable velocity by 70 discrete velocity points. The collision operators $\mathcal{L}$ in Eq. (3) are replaced by integrals over kernels using Eq. (4); they in turn appear as 70×70 matrices in the discrete rate equations. These equations have been solved on a IBM 3083 JX main frame which needs 8 sec processor time for a single run yielding the velocity distributions in all four levels for one set of input parameters.

All spectroscopic and collisional Na parameters have been chosen to have the same values as in Ref. 30. In this context the transit relaxation deserves some comment. We use the standard result[30]

$$\Gamma_T = \frac{(2.405)^2 D_g}{R^2} \left[\frac{1}{1 + K/p} \right] . \quad (6)$$

Here R is the radius of the laser beam, D_g is the diffusion coefficient of ground-state Na atoms at the prevailing perturber pressure, 2.405 is the lowest zero of the zeroth-order Bessel function, and K is a Knudsen coefficient defined as

$$K = c \frac{\bar{l} p}{R} . \quad (7)$$

Here $\bar{l}$ is the mean-free path and c is a numerical constant which is equal to 6.8 for a hard-sphere interaction. Equation (6) is valid for the whole pressure range, including the Knudsen limit. In the latter limit, it reduces to $T = \bar{v}/2R$ which is simply the reciprocal time of flight of a Na atom through the laser beam. In the rate equations, transit relaxation has the same effect on the velocity distributions as strong velocity-changing collisions, i.e., collisions which thermalize the velocity distribution. However, the transit relaxation is inversely proportional (through D_g) to the buffer gas pressure p as long as $p \gg K$, whereas the collision rate is linearly proportional to p. As an example, in the case of Xe as a buffer gas, the velocity-changing collisions are strong and one finds, using Eq. (6) together with data for the collision rate,[30] that

$$\frac{\Gamma_T}{\Gamma_g^{\rm vcc}} = \frac{6\times 10^{-3}}{(pR)^2} \quad (p \text{ in Torr, } R \text{ in mm}) , \tag{8}$$

where $\Gamma_g^{\rm vcc}$ is the rate for velocity-changing collisions in the ground state. In most practical cases for LID, $pR \gg 0.1$ mm Torr so that the transit relaxation is negligible. Clearly, in the limit that the pressure becomes small ($pR < 0.1$ mm Torr), the transit relaxation cannot be neglected (see below). In the examples we have chosen $R = 1$ mm, this being a typical experimental value.[25,27–29]

We have tested the computer code by calculating several limiting cases as to the buffer gas pressure p and the rates for velocity-changing collisions. Specifically, the cases $p \to 0$, $p \to \infty$, and $\Gamma_0^{\rm vcc} = \Gamma_1^{\rm vcc} = \Gamma_2^{\rm vcc} = \Gamma_3^{\rm vcc}$ all yielded a zero drift velocity, as expected. Moreover, we have simulated numerically the analytical two-level theory[6,8,12] by collapsing the splittings Δ_{12} and Δ_{03} and compared our numerical results with the analytical ones; this yielded an error bar of 10% for the numerical results.

A. LID as a function of laser detuning

The single-level contributions $v_{\rm dr}^{(i)}$ to the total drift velocity are shown in Fig. 3(a) for the case Na-Ar as a function of the laser detuning. It is clear that the magnitude of the total drift velocity is determined by almost cancelling contributions from atoms in all four levels. This shows that a complete four-level description is indeed essential for the description of LID in Na-buffer-gas mixtures.

Figure 3(b) shows the corresponding single-level populations n_i/n as a function of laser detuning. The complementarity of the populations in the ground-state hyperfine levels ($F = 1,2$) is due to the process of optical hyperfine pumping.[32] In order to illustrate this process, let us assume that the laser frequency is tuned into the red Doppler wing of the $2 \to 0$ transition. In that case the laser will dominantly excite atoms in the $F = 2$ hyperfine level, which after excitation will decay spontaneously to both the $F = 1$ and $F = 2$ hyperfine ground-state level, in the ratio 3:5. Since the rate for direct collision-induced transfer between both hyperfine levels is extremely small (cross section[33] smaller than 10^{-20} cm^2), the Na atoms will end up in the $F = 1$ hyperfine ground-state level after a few pump cycles. Therefore, the absorption of light and the drift velocity will be drastically reduced. Fortunately, the Na atoms are not completely pumped to the nonresonant $F = 1$ ground-state level so that the drift will not vanish. In the first place, thermalized Na atoms, which might, for instance, have undergone hyperfine relaxation during a wall collision, diffuse into the laser beam (transit relaxation). This is, however, a negligible effect in practical cases; a simple estimate shows that the transverse diffusion rate is many orders of magnitude smaller than the excitation rate. In the second place, the laser also excites Na atoms in the collisional wing of the $1 \to 0$ transition. This "back pumping" is the major factor determining the relative steady-state populations of the ground-state levels $F = 1$ and $F = 2$ and thus has important consequences for the drift velocity. Additionally,

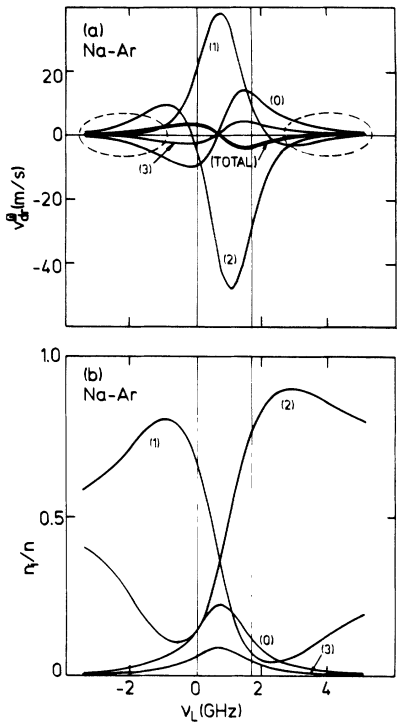

FIG. 3. (a) Calculated single-level contributions to the drift velocity and (b) the corresponding level populations as a function of laser detuning relative to the $2 \to 0$ (i.e., $^2S_{1/2}$, $F = 2 \to {}^2P_{3/2}$) transition. The two thin vertical lines indicate the $F = 1$ and $F = 2$ hyperfine components. The conditions correspond to 10-Torr Ar and a laser intensity of 10 W/cm^2. The heavy curve in (a) represents the total drift velocity. The encircled regions denote the approximate validity region of the homogeneous two-level limit.

since the hyperfine splitting of the ground state is of the order of the Doppler width, also the $1 \to 0$ excitation is somewhat velocity selective and therefore contributes to the drift as well [see Fig. 3(a)].

The incorporation of the effect of optical hyperfine pumping is the most important aspect of the four-level description as compared to a two-level approach. In order to illustrate the importance of optical hyperfine pumping for LID we compare in Fig. 4 the calculated frequency dependence of the drift velocity for the cases that the ground-state hyperfine splitting has been set to 0 GHz [curve (*a*)] and to its proper value of 1.77 GHz [curve (*b*)], respectively, using the same set of input parameters. It is evident that the magnitude of the drift velocity is strongly affected; the drift velocity decreases by a factor of 4 for excitation in the Doppler core of the transition. The deviation of curve (*b*) from the antisymmetric shape is a consequence of the fact that the two ground-state hyperfine levels have different degeneracies.

The role of the excited-state fine-structure splitting is found to be much less important. For example, if we neglect fine-structure-mixing collisions in the case (*a*) of Fig. 4, thus performing actually a two-level calculation, the calculated drift velocities differ by no more than a few

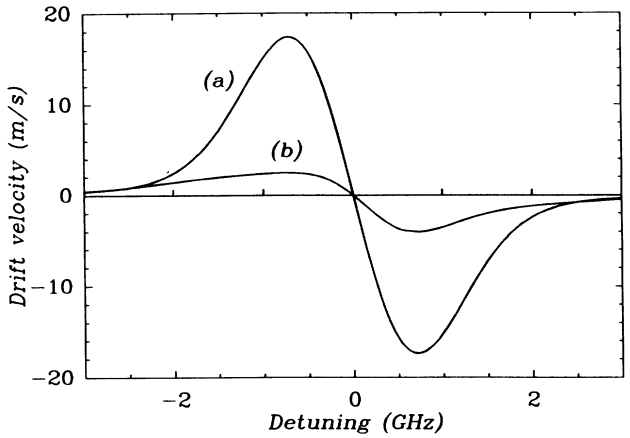

FIG. 4. Calculated drift velocity of Na in Xe as a function of laser detuning. We have set the ground-state hyperfine splitting to 0 GHz [curve (*a*)] and to its proper value of 1.77 GHz [curve (*b*)]. The buffer gas pressure is 1.0 Torr and the laser intensity is 10 W/cm^2. For sake of comparison curve (*a*) has been shifted 0.57 GHz along the frequency axis, so that the points where the drift velocity changes sign coincide. The large difference between the two curves is due to optical hyperfine pumping.

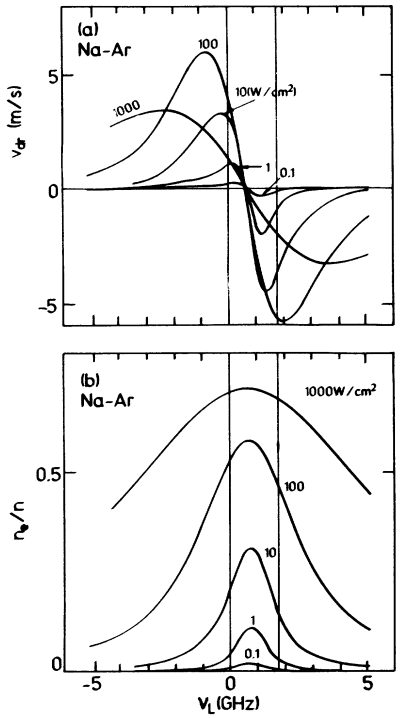

FIG. 5. (a) Calculated drift velocity and (b) excited-state fraction at 10-Torr Ar as a function of the laser detuning relative to the $2\rightarrow 0$ (i.e., $^2S_{1/2}$, $F=2\rightarrow 2\,^2P_{3/2}$) transition. The two thin vertical lines indicate the $F=1$ and $F=2$ hyperfine components. The excited-state fraction as a function of laser detuning represents in fact the absorption spectrum. The curves correspond to laser intensities of 0.1, 1, 10, 100, 1000 W/cm^2. It is seen that the shape of the drift velocity spectrum is roughly proportional to the first derivative of the absorption spectrum.

percent from those shown in curve (*a*).[34]

Examples of the calculated spectral dependence of the total drift velocity are shown in Fig. 5(a) for the case of Na-Ar for several values of the laser intensity. At high intensities power broadening is larger than the hyperfine splitting so that the drift velocity spectrum becomes perfectly antisymmetric. The corresponding spectral dependences of the excited-state population $n_e \equiv n_0 + n_3$ are shown in Fig. 5(b); they are proportional to the absorption spectra. It can be shown[35] that the drift velocity spectrum in a two-level system is proportional to the first derivative of the absorption spectrum (a Voigt profile) provided that saturation is negligible and provided that one uses a strong collision model. For a four-level system, due to the "saturation" associated with optical hyperfine pumping, there is no justification for a similar relation between the drift velocity and the absorption spectrum. However we observe from Fig. 5 that the drift velocity spectrum in a four-level system is still roughly proportional to the first derivative of the absorption spectrum. A closer inspection reveals that this relation is not exactly valid. All drift velocity spectra cross zero at a detuning $(\nu_L - \nu_{20}) \sim 0.6$ GHz; at this frequency the drift of Na atoms excited from the $F=2$ level compensates the drift of those excited from the $F=1$ level. The absorption spectrum reaches its maximum at $(\nu_L - \nu_{20}) \sim 0.8$ GHz.

Further numerical analysis[23] shows that in the case of a four-level system the drift velocity spectrum is still roughly proportional to the first derivative of the absorption spectrum if the ground-state hyperfine splitting is not appreciably larger than the Doppler width, a condition which is indeed valid for the case of Na. In this case optical hyperfine pumping is relatively mild. This approximate proportionality is violated when the ground-state hyperfine splitting becomes larger than the Doppler width, as is the case for Rb.[23,24,26] In this case optical hyperfine pumping is severe. Similar considerations have been brought forward by Parkhomenko and Shalagin.[5]

B. LID as a function of the laser intensity

In Figs. 6(a) and 6(b) we present results for the intensity dependence of the drift velocity for several values of the buffer gas pressure and the laser detuning, respectively. We observe that the intensity dependence of the drift velocity has a nearly universal functional dependence: a "bell-shaped" curve is observed if we use a logarithmic intensity scale. For each curve one can distinguish various regimes. At intensities smaller than the homogeneous saturation intensity ($I < 0.01$ W/cm^2, not shown in Fig. 6) the drift velocity increases linearly with increasing intensity, since more and more Na atoms in the resonant velocity class are excited. For larger intensities the Na atoms are inhomogeneously saturated, leading to a sublinear dependence of the drift velocity on the intensity; the drift velocity keeps increasing with intensity, since the width of the excited velocity class increases due to power broadening. For even larger intensities the drift velocity goes through a maximum when due to power

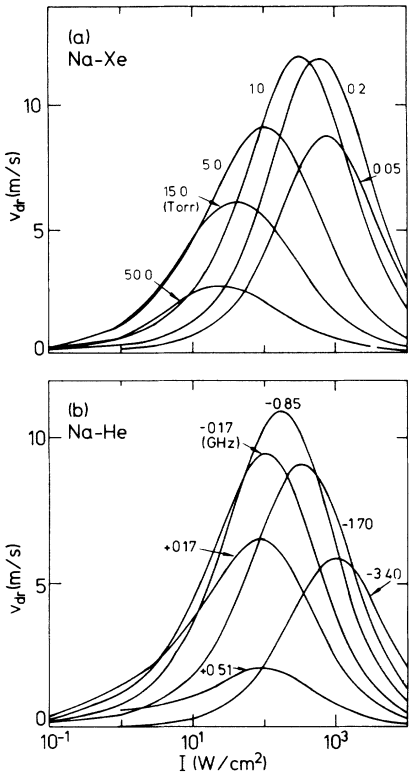

FIG. 6. (a) Calculated drift velocity as a function of laser intensity for several buffer gas pressures (0.05-, 0.2-, 1.0-, 5-, 15-, 50-Torr Xe) for a laser detuning of -0.17 GHz relative to the $2\rightarrow0$ (i.e., $^2S_{1/2}$, $F=2\rightarrow2\,^2P_{3/2}$) transition (i.e., in the red wing). (b) Calculated drift velocity as a function of laser intensity for 5-Torr He and laser detunings of $+0.51$, $+0.17$, -0.17, -0.85, -1.70, and -3.40 GHz relative to the $2\rightarrow0$ transition.

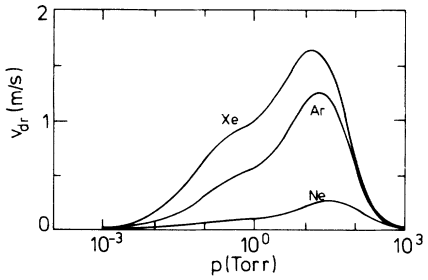

FIG. 7. Calculated pressure dependence of the drift velocity for Na in Ne, Ar, or Xe at a laser intensity of 3 W/cm^2, a laser detuning of -0.85 GHz relative to the $2\rightarrow0$ (i.e., $^2S_{1/2}$, $F=2\rightarrow{}^2P_{3/2}$) transition and a laser beam diameter of 2 mm.

broadening atoms going in the "wrong" direction are also excited. Finally, when the intensity becomes such that the whole Doppler profile is saturated all velocity selectivity is lost and the drift velocity vanishes.

The maximum drift velocity as a function of intensity is denoted as v_{dr}^{max} and the intensity at which this maximum occurs as I_{max}. It can be seen from Figs. 6(a) and 6(b) that v_{dr}^{max} is only weakly dependent on the buffer gas pressure and the laser detuning: v_{dr}^{max} varies less than a factor of 2 for pressures between 0.05 and 15 Torr and detuning, between $+0.17$ GHz and -3.40 GHz relative to the $2\rightarrow0$ transition. Although the shape of $v_{dr}(I)$ and the value v_{dr}^{max} are relatively independent of pressure and detuning, the intensity I_{max} required to obtain v_{dr}^{max} is strongly dependent on the experimental conditions: one needs only 30 W/cm^2 to reach the maximum drift velocity at a small detuning (-0.17 GHz) and a high buffer gas pressure (50 Torr), but much higher intensities are required at lower pressures or larger detunings.

C. LID as a function of buffer gas pressure

The calculated dependence of the drift velocity on the noble-gas pressure is shown in Fig. 7 for a laser intensity of 3 W/cm^2 and a laser detuning of -0.85 GHz. In this case the drift velocity is maximum for a noble-gas pressure of $\sim$20 Torr. For pressures above 20 Torr the drift velocity decreases due to increasing kinetic thermalization during a radiative lifetime and also due to the fact that the homogeneous linewidth increases to values on the order of the Doppler width. For pressures below 20 Torr the drift velocity decreases due to two mechanisms. The first of these is active between 20 and 1 Torr. In this region the pressure dependence is due to the fact that the laser is not only resonant with the $2\rightarrow0$ transition, but also excites the $1\rightarrow0$ transition in its collisional wing, pumping atoms back from level 1 to level 0, thus (partly) defeating the optical hyperfine pumping cycle as was explained in Sec. III A. This back pumping mechanism becomes less effective at low pressure, leading to a decreasing drift velocity at decreasing pressure. Below 1 Torr, the drift velocity starts to decrease again due to a second mechanism: the probability that an excited atom suffers a collision with a buffer gas atom inside the laser beam decreases from unity to zero. This second mechanism is a consequence of the transit relaxation term introduced in Sec. II.

In previous theories of LID[2,6,8,12] the drift velocity generally approaches a maximum value in the limit of vanishing buffer gas pressure. This result is due to the fact that it is (implicitly) assumed in those theories that the size of the system (i.e., the vapor cell) is much larger than the atomic mean-free path, i.e., the system should be infinitely large in the limit of vanishing buffer gas pressure. If one adopts a finite experimental system the drift velocity goes to zero in the low pressure limit, as shown in Fig. 7.

In Fig. 8 we present the calculated contribution of each individual Na level to the total drift velocity $v_{dr}^{(i)} = \int v_z f_i(v_z)\,dv_z$ as a function of the buffer gas pressure; the heavy curve represents the total drift velocity which can be observed experimentally. Figures 8(a) and 8(b) correspond to laser intensities of 30 W/cm^2 and 400 W/cm^2, respectively. Note that the single-level contribution $v_{dr}^{(i)}$ is not to be confused with the average velocity of atoms in level i which is given by $v_{dr}^{(i)}/n_i$. As before (see Fig. 3) we observe that all four levels contribute (with different signs) to the total drift velocity; in fact, all

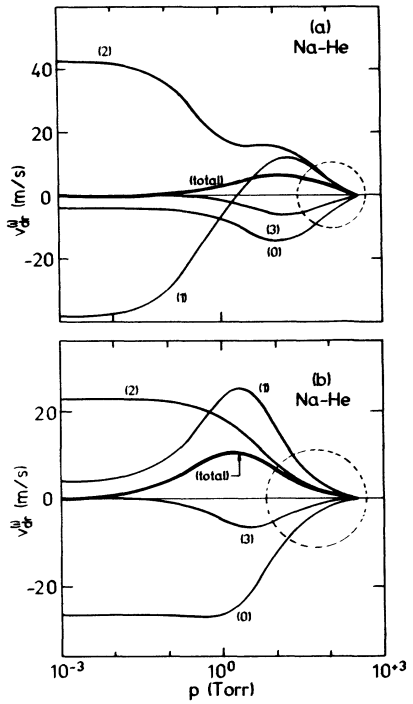

FIG. 8. Calculated single-level contributions to the drift velocity in combination with the total drift velocity (heavy curve) as a function of the He pressure. The laser detuning is -0.85 GHz relative to the $2\rightarrow 0$ transition (i.e., $^2S_{1/2}$, $F=2\rightarrow {}^2P_{3/2}$) and the laser intensity is (a) 30 W/cm^2 or (b) 400 W/cm^2. The encircled regions denote the approximate validity region of the homogeneous two-level limit.

single-level contributions to the drift velocity are of the same order of magnitude, and generally are much larger than the total drift velocity. It is seen in Figs. 8(a) and 8(b) that for large saturation-broadened homogeneous linewidths, both ground-state hyperfine levels yield comparable contributions to the drift velocity. The same statement applies to the contributions from both excited-state fine structure levels. This is an indication that the homogeneous two-level limit[6] starts to become valid for large values of the saturation-broadened homogeneous linewidth. In Fig. 8 the encircled regions indicate the approximate validity region of this limit.

D. Dependence on the noble gas

In Table I we summarize the relative difference between the ground-state and excited-state rate for velocity-changing collisions $(\Gamma_e^{\rm vcc}-\Gamma_g^{\rm vcc})/\Gamma_g^{\rm vcc}$ and the calculated maximum attainable drift velocities for each noble gas. It should be noted that this latter quantity is not identical to $v_{\rm dr}^{\rm max}$ (as introduced in Sec. III B) which is still a function of p and ν_L. The maximum value of $v_{\rm dr}^{\rm max}$ has been found for each noble gas as the result of an extensive numerical search in which we have varied p, ν_L, and I_L. It is found that a drift velocity of 13.8 m/s can be achieved using Xe as a buffer gas. We observe that the

TABLE I. The maximum obtainable drift velocity in each Na–noble-gas mixture for optimum choice of noble-gas pressure, laser intensity, and laser detuning. It can be seen that the maximum obtainable drift velocity is roughly proportional to the relative difference between the rates for velocity-changing collisions in the ground and the excited states.

	$\frac{\Gamma_e^{\rm vcc}-\Gamma_g^{\rm vcc}}{\Gamma_g^{\rm vcc}}$	Maximum drift velocity (m/s)
He	+0.35	10.8
Ne	+0.04	1.43
Ar	+0.26	8.04
Kr	+0.42	12.2
Xe	+0.49	13.8

maximum attainable drift velocity is approximately proportional to $(\Gamma_e^{\rm vcc}-\Gamma_g^{\rm vcc})/\Gamma_g^{\rm vcc}$ as is the case in a naive two-level description of LID. The experimental conditions required to obtain the maximum drift velocity can be deduced from Figs. 9(a) and 9(b). In these figures we present the calculated drift velocity for all Na–noble-gas

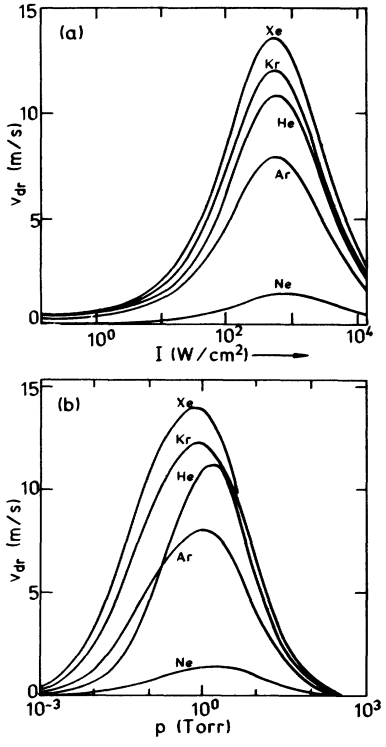

FIG. 9. (a) Calculated drift velocity as a function of laser intensity for all Na–noble-gas pairs, at a pressure of 1 Torr and a detuning of -0.85 GHz relative to the $2\rightarrow 0$ (i.e., $^2S_{1/2}$, $F=2\rightarrow {}^2P_{3/2}$) transition. This pressure and detuning correspond approximately to the maximum attainable drift velocity for each Na–noble-gas pair. (b) Calculated drift velocity as a function of pressure for all Na–noble-gas pairs at a laser intensity of 600 W/cm^2 and a detuning of -0.85 GHz relative to the red wing of the $2\rightarrow 0$ transition. This laser intensity and detuning correspond approximately to the maximum attainable drift velocity for each Na–noble-gas pair.

pairs as a function of laser intensity and as a function of pressure, respectively. For all Na–noble-gas pairs the maximum drift velocity is realized at a laser intensity of ~ 600 W/cm^2, a laser detuning $\nu_L - \nu_L(v_{dr}=0) = \pm 1.45$ GHz and a buffer gas pressure of ~ 1 Torr. Here $\nu_L(v_{dr}=0)$ is the laser frequency for which the drift velocity changes sign [see Sec. III A and Fig. 5(a)].

E. Influence of the collision kernel

As discussed above, in our model we describe velocity-changing collisions by means of a composite Keilson-Storer kernel which contains both a large-angle part and a small-angle part. Figure 10 shows the calculated velocity distribution in the resonant excited-state level (level 0) for three different noble gases at identical "experimental" conditions. The major difference between these cases is in the shape of the large-angle Keilson-Storer kernel, which is relatively weak ($\alpha^{KS-LA}=0.8$) for Na-He, intermediate ($\alpha^{KS-LA}=0.2$) for Na-Ar, and strong ($\alpha^{KS-LA}=0$ for Na-Xe. It is seen in Fig. 10 that the shape of the velocity distribution in level 0 reflects the shape of the collision kernel.

In Fig. 11 the calculated drift velocity is presented as a function of pressure. We have used in this case Na-He parameters, apart from the strength parameter $\alpha_g^{KS-LA}=\alpha_e^{KS-LA}$ of the Keilson-Storer kernel for LA scattering, which in this case is considered to be a free parameter; the cases $\alpha^{KS-LA}=0$ and $\alpha^{KS-LA}=0.95$ are shown (note that the latter choice corresponds in fact to rather weak collisions). Laser intensity and detuning correspond to a typical experiment.[25–29,36] While varying α^{KS-LA} the product $(1-\alpha^{KS-LA})\Gamma^{KS-LA}$, which is proportional to the diffusion cross section,[37] was kept constant. It is seen from Fig. 11 that, quite surprisingly, the drift velocity is not sensitive to the shape of the Keilson-Storer kernel, although the underlying velocity distributions are clearly affected by the shape of the kernel as is shown in Fig. 10. Our observations that the drift velocity is independent of the Keilson-Storer strength parameter α^{KS-LA} can be justified by the analytical two-level treatment of Kryszewski and Nienhuis[11] who used a Keilson-Storer collision model. Inspection of Eqs. (68)–(71) in that work also shows that the drift velocity is primarily dependent on the difference between the values of $(1-\alpha)\Gamma$ for the ground state and the excited state.

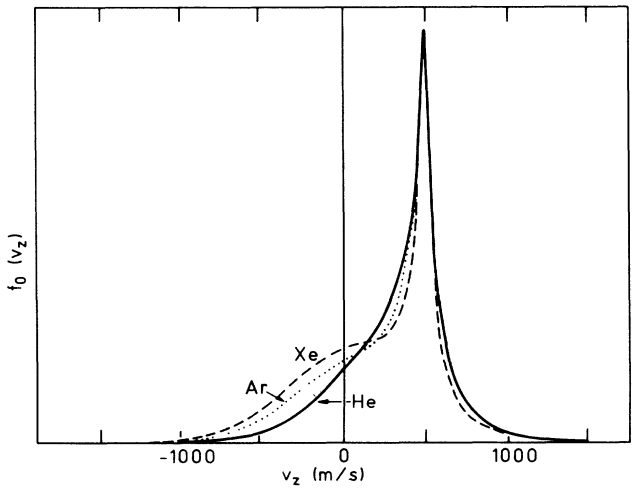

FIG. 10. Calculated velocity distribution in the resonant excited-state fine-structure level for Na-He, Na-Ar, and Na-Xe at a laser intensity of 0.3 mW/cm^2, a detuning of -0.85 GHz relative to the $2\rightarrow 0$ (i.e., $^2S_{1/2}$, $F=2\rightarrow {}^2P_{3/2}$) transition and a buffer gas pressure of 5 Torr.

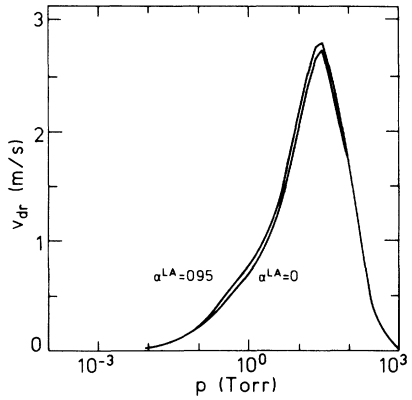

FIG. 11. Calculated pressure dependence of the drift velocity for two different assumed Keilson-Storer kernels. Parameters used are those for Na-He apart from the value of the large-angle Keilson-Storer strength which is considered to be free. Results are shown for two values: $\alpha^{KS-LA}=0.0$ which corresponds to strong collisions and $\alpha^{KS-LA}=0.95$, which corresponds to relatively weak collisions. The Keilson-Storer collision rate Γ has been chosen such that the product $(1-\alpha^{KS-LA})\Gamma^{KS-LA}$ is the same for the two cases; this product is proportional to the diffusion cross section. The results shown correspond to a laser intensity of 3 W/cm^2 and a detuning of -0.85 GHz relative to the $2\rightarrow 0$ (i.e., $^2S_{1/2}$, $F=2\rightarrow {}^2P_{3/2}$) transition.

The dependence of the drift velocity on the small-angle kernel for excited-state collisions has been studied by varying α_e^{KS-SA} between its experimentally obtained value[30] and $\alpha_e^{KS-KS}=1.0$; the latter value of α_e^{KS-SA} corresponds to the absence of small-angle scattering. We found that the variation of the drift velocity due to the variation of α_e^{KS-SA} was completely negligible, showing that the drift velocity is also not sensitive to small-angle scattering.

We conclude that the drift velocity is not at all sensitive to the shape of the collision kernel for velocity-changing collisions. Apparently the details of the collisional interaction do not survive the integration contained in Eq. (1). In fact, the drift velocity is only dependent on the level-dependent diffusion cross sections which determine the product $(1-\alpha^{KS-LA})\Gamma^{KS-LA}$, irrespective of the values of α^{KS-LA} and Γ^{KS-LA} separately. More specifically, the difference between the excited-state and the ground-state diffusion cross sections determines the drift velocity. The latter cross sections have been calculated for all Na–noble-gas pairs within the framework of

the sudden approximation, using calculated or measured interaction potentials.[38]

IV. SUMMARY AND CONCLUSIONS

We have presented, for the first time, realistic model calculations for LID in a Na–noble-gas system. Our calculations include the multilevel aspects of the Na atom, the effects of strong saturation, the transit relaxation term, and a realistic collision model. It has been shown that our description of LID of Na in a noble-gas environment leads to qualitatively different behavior of the drift velocity as compared with predictions on the basis of previous work.[4–12] By calculating the single-level contributions to the total drift velocity, it has been shown that all levels contribute to LID, implicating that a four-level description is essential for most practical experimental conditions. The hyperfine splitting of the ground state can have a large effect on LID via optical hyperfine pumping; the fine-structure splitting of the excited state has much less effect. The larger part of our model calculations can be directly verified experimentally in the "optical machine gun" configuration;[27] preliminary experiments show good agreement[28] and more work will follow shortly.[39] Verification of the effects of transit relaxation and observation of the maximum of the drift velocity as a function of intensity will require capillary diameters smaller than used so far (1–2 mm) and/or sharply focused laser beams.

We have also found that the drift velocity in Na–noble-gas mixtures is only determined by the difference in diffusion coefficient between the ground-state and the excited-state, while the details of the collision model do not influence the drift velocity significantly. We conclude that for the calculation of the drift velocity, it suffices to use the strong collision model, provided that one chooses the cross section for velocity-changing collisions equal to the diffusion cross section. Due to the latter result, our rate-equation model, capable to describe both the macroscopic LID phenomenon and the underlying single-level velocity distributions,[30] can be simplified considerably in a straightforward manner, when one is interested only in the macroscopic drift velocity.

The maximum attainable drift velocity of Na in a noble gas is predicted to be 13.8 m/s for the case of Na-Xe. However, it should be noted that this is the maximum drift velocity for the case of a single monochromatic laser field. Higher drift velocities can be obtained when a multifrequency laser is used[27] or when two single-frequency lasers are used with a frequency spacing of the order of the hyperfine splitting of the ground state.[28] We expect that by suitable spectral tailoring of the laser field, the maximum attainable drift velocities will approach those which can be reached in a two-level system. The case of two-frequency or multifrequency excitation can be easily incorporated in our numerical model.[28,39]

Finally, we note that the model can be extended to other systems, e.g., other alkali-metal–noble-gas systems. In particular, the Rb–noble-gas system[23,24,26] seems to be an attractive candidate for LID since (i) the two isotopes of Rb can be separated by LID[23,24] and (ii) the drift velocity in a Rb–noble-gas system should reverse sign when the laser is tuned from the D_1 line to the D_2 line.[26,38] For the case of Rb (and also Cs) the excited-state collisions should be treated in the adiabatic approximation instead of the sudden approximation since in that case the fine-structure splitting is much larger than in the case of Na.

ACKNOWLEDGMENTS

We thank G. Nienhuis, P. R. Berman, and I. Kuščer for stimulating discussions. This work is part of the research program of the Foundation for Fundamental Research on Matter (FOM) and was made possible by financial support of the Netherlands Organization for Scientific Research (NWO).

---

*Present address: Department of Physics, Eindhoven University of Technology, P.O. Box 513, 5600 MB Eindhoven, The Netherlands.

†Present address: Joint Institute for Laboratory Astrophysics, University of Colorado, Box 440, Boulder, CO 80309.

[1] F. Kh. Gel'mukhanov and A. M. Shalagin, Pis'ma Zh. Eksp. Teor. Fiz. **29**, 773 (1979) [JETP Lett. **29**, 711, (1979)].

[2] F. Kh. Gel'mukhanov and A. M. Shalagin, Zh. Eksp. Teor. Fiz. **78**, 1674 (1980) [Sov. Phys.—JETP **51**, 839 (1980)].

[3] F. Kh. Gel'mukhanov and G. G. Telegin, Zh. Eksp. Teor. Fiz. **80**, 974 (1981) [Sov. Phys.—JETP **53**, 495 (1981)].

[4] V. R. Mironenko and A. M. Shalagin, Izv. Akad. Nauk. SSSR, Ser. Fiz. **45**, 995 (1981) [Bull. Acad. Sci. USSR, Phys. Ser. **45**, 87 (1981)].

[5] A. I. Parkhomenko and A. M. Shalagin, Physica **142C**, 120 (1986).

[6] F. Kh. Gel'mukhanov, J. E. M. Haverkort, S. W. M. Borst, and J. P. Woerdman, Phys. Rev. A **36**, 164 (1987).

[7] S. Zielińska, J. Phys. B **18**, 1333 (1985).

[8] G. Nienhuis, Phys. Rep. **138**, 151 (1986).

[9] F. Kh. Gel'mukhanov, L. V. Il'ichov, and A. M. Shalagin, J. Phys. A **19**, 2201 (1987).

[10] F. Kh. Gel'mukhanov, L. V. Il'ichov, and A. M. Shalagin, Physica **137A**, 502 (1986).

[11] S. Kryszewski and G. Nienhuis, J. Phys. B **20**, 3027 (1987).

[12] F. Kh. Gel'mukhanov, Izv. VUZ. Avtometriya **1**, 49 (1985) [Optoelectron. Instrum. Data Proc. **1**, 43 (1985)].

[13] F. Kh. Gel'mukhanov and L. V. Il'ichov, Phys. Lett. **103A**, 61 (1984).

[14] F. Kh. Gel'mukhanov, Kvant. Elektron. **11**, 510 (1984) [Sov. J. Quantum Electron. **14**, 347 (1984)].

[15] A. V. Gainer, K. P. Komarov, and K. G. Folin, Zh. Eksp. Teor. Fiz. **82**, 1853 (1982) [Sov. Phys.—JETP **55**, 1068 (1982)].

[16] A. K. Folin, K. G. Folin, A. V. Ghiner, and K. P. Komarov, Opt. Commun. **40**, 129 (1981).

[17] S. N. Atutov, I. M. Ermolaev, and A. M. Shalagin, Pis'ma Zh. Eksp. Teor. Fiz. **40**, 374 (1984) [JETP Lett. **40**, 1188 (1984)].

[18] E. M. Skok and A. M. Shalagin, Pis'ma Zh. Eksp. Teor. Fiz.

32, 201 (1980) [JETP Lett. **32**, 184 (1980)].

[19]A. F. Kravchenko, A. M. Palkin, V. N. Sozinov, and O. A. Shegaĭ, Pis'ma Zh. Eksp. Teor. Fiz. **38**, 328 (1983) [JETP Lett. **38**, 393 (1983)].

[20]V. D. Antsygin, S. N. Atutov, F. Kh. Gel'mukhanov, G. G. Telegin, and A. M. Shalagin, Pis'ma Zh. Eksp. Teor. Fiz. **30**, 262 (1979) [JETP Lett. **30**, 243 (1979)]; A. D. Antsigin, S. N. Atutov, F. Kh. Gel'mukhanov, A. M. Shalagin, and G. G. Telegin, Opt. Commun. **32**, 237 (1980).

[21]V. N. Panfilov, V. P. Strunin, P. L. Chapovskiĭ, and A. M. Shalagin, Pis'ma Zh. Eksp. Teor. Fiz. **33**, 52 (1981) [JETP Lett. **33**, 48 (1981)].

[22]A. K. Folin and P. L. Chapovskiĭ, Pis'ma Zh. Eksp. Teor. Fiz. **38**, 452 (1983) [JETP Lett. **38**, 549 (1983)].

[23]A. D. Streater, J. Mooibroek, and J. P. Woerdman, Opt. Commun. **64**, 137 (1987).

[24]A. D. Streater, J. Mooibroek, and J. P. Woerdman, Appl. Phys. Lett. **52**, 602 (1988).

[25]H. G. C. Werij, J. P. Woerdman, J. J. M. Beenakker, and I. Kuščer, Phys. Rev. Lett. **52**, 2237 (1984).

[26]W. A. Hamel, A. D. Streater, and J. P. Woerdman, Opt. Commun. **63**, 32 (1987).

[27]S. N. Atutov, St. Lesjak, S. P. Podjachev, and A. M. Shalagin, Opt. Commun. **60**, 41 (1986).

[28]H. G. C. Werij, J. E. M. Haverkort, P. C. M. Planken, E. R. Eliel, J. P. Woerdman, S. N. Atutov, P. L. Chapovskii, and F. Kh. Gel'mukhanov, Phys. Rev. Lett. **58**, 2660 (1987).

[29]J. H. Xu, M. Allegrini, S. Gozzini, E. Mariotti, and L. Moi, Opt. Commun. **63**, 43 (1987).

[30]J. E. M. Haverkort, J. P. Woerdman, and P. R. Berman, Phys. Rev. A **36**, 5251 (1987).

[31]J. E. M. Haverkort, Ph. D. thesis, University of Leiden, 1987; J. E. M. Haverkort and J. P. Woerdman, in *Laser Spectroscopy*, Proceedings of the XV Summer School on Quantum Optics, edited by J. Heldt and R. Lawruszuk (World Scientific, Singapore, 1987).

[32]R. Walkup, A. Spielfiedel, W. D. Phillips, and D. E. Pritchard, Phys. Rev. A **23**, 1869 (1981).

[33]W. Happer, Rev. Mod. Phys. **44**, 169 (1972).

[34]In the four-level model the excited-state diffusion cross section is independent of the fine-structure level as a consequence of the sudden approximation.

[35]A. E. Bakarev and A.K. Folin, Opt. Spektrosk. **62**, 475 (1987) [Opt. Spectrosc. **62**, 284 (1987)].

[36]H. G. C. Werij, J. E. M. Haverkort, and J. P. Woerdman, Phys. Rev. A **33**, 3270 (1986).

[37]P. R. Berman, J. E. M. Haverkort, and J. P. Woerdman, Phys. Rev. A **34**, 4647 (1986).

[38]W. A. Hamel, J. E. M. Haverkort, H. G. C. Werij, and J. P. Woerdman, J. Phys. B **19**, 4127 (1986),

[39]H. G. C. Werij, Ph. D. thesis, University of Leiden, 1988; H. G. C. Werij and J. P. Woerdman, Phys. Rep. **169**, 145 (1988).